

Automatic Extraction and Localisation of Optic Disc in Colour Fundus Images

Thresiamma Devasia¹, Poulouse Jacob² and Tessamma Thomas³

¹ Department of Computer Science
Assumption College ,
Changanacherry, Kerala State, Kottayam, India

² Department of Computer Science, Cochin University of Science and Technology
Cochin, Kerala State, Cochin, India

³ Department of Electronics, Cochin University of Science and Technology
Cochin, Kerala State, Cochin, India

Abstract

The color fundus images are used to track eye diseases by the ophthalmologists and it provides early signs of certain diseases such as diabetes. The optic disc extraction and segmentation is essential for the detection of many retinal diseases. The automatic screening facility helps the ophthalmologist to save time for the symptom detection. This paper presents a new histogram based multilevel thresholding method to segment and extract optic disc from colour fundus images. In this method, a hill-clustering technique is applied to the vessel free image histogram in order to determine the peak locations of the histogram and the histogram segments between the peaks are fitted by real rational functions. Finally, the multi level threshold values of the histogram are defined as the global minimum values of each rational function. This is an efficient technique for the segmentation because it is applicable to the value of image histogram directly to recognize the absolute transition point. The method was tested on a total of 404 images from publically available databases DRION, DIARETDB0 and DIARETDB1 and, also images collected from an ophthalmologist. The success rate of this method is 96.78%. The performance of the method was evaluated using the difference in centroid of the obtained optic disc and that of the ground truth obtained from an expert ophthalmologist. From the scatter plot, it is shown that the ground truth and detected optic disc centers have a high positive correlation.

Keywords: fundus image, optic disc, multilevel thresholding, local minima, global minima

1. Introduction

The retina is a part of the posterior segment of the eye, called fundus. Images of ocular fundus (fundus images) can help in diagnosis and treatment of many diseases including various retinopathies, ophthalmic pathologies, glaucoma etc. The optic disc (OD) is considered to be a very

important feature in a retinal fundus image. Optic nerve head (ONH) evaluation is important for the early detection of many retinal diseases. Changes in the structural appearance of the OD are usually used for the symptom detection of different diseases. Hence, cautious documentation of optic nerve morphometric parameters [1]. Figure 1 depicts the main features of a fundus eye image such as optic disc, optic cup and blood vessels.

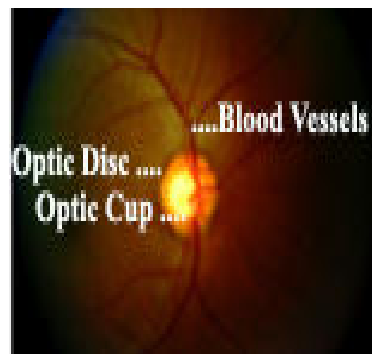


Figure1. A colour Fundus image

The OD extraction and localisation are important steps in many systems. Localised images are used in different applications like diagnosis, treatment planning, localization of pathology etc. OD localisation, however, is a difficult task due to variation of OD shape and image quality. Precise and reproducible measurements of OD are also critically important for evaluating the progression of certain diseases like glaucoma. Automatic OD localization is a critical step in eye image processing, since it serves as a landmark for subsequent diagnostics. Although various disparities in ODs are seen among people, they are

typically characterized by their nearly circular shape and also as the convergence region of a network of blood vessels and nerves [2].

2. Related work

Hoover A. et al. [2] developed an automated method to locate the optic nerve in fundus images. They used fuzzy convergence to determine the origination of the blood vessel network. H. Li et al.[3] presented a method based on a point distribution shape model of OD boundary which is derived from training images. The learned shape model is integrated with deformable contour model to obtained OD boundary. Lowell et al. [4] uses a elliptical shape based deformable model to extract OD boundary. Hough transform was used for OD detection by Chrastek et al. [5]. Seng et al. [6] have used the unsupervised color thresholding technique for optic disk detection. Yandong Tang et al. [7] presented an automatic segmentation of the papilla in a fundus image based on the Chan-Vese model and a shape restraint. The experimental results show that this method shows a good performance in detecting the papilla shapes and computing the shape feature parameters.

Virance et al. [8] have detected the optical disk from low contrast images using deformable model based approach. A unified deformable contour approach for OD and cup boundary detection is presented by J. Xu et al.[9]. D.W.K. Wong et al.[10] presented a variational level set method for disc segmentation. An ellipse fitting is also used here for boundary smoothing. Jun Cheng et al. [11] did the automatic optic disc segmentation with peripapillary atrophy elimination. Handayani Tjandrasa et al. [12] developed a method for OD segmentation using hough transform and active contour operations.

3. Developed Method

3.1 New Algorithm

Thresholding often provides an easy and convenient way to perform the segmentation on the basis of the different intensities or colors in the foreground and background regions of an image. Multilevel thresholding is one of the most powerful techniques for image segmentation. The application of multilevel thresholding techniques is based on the assumption that object and background pixels in a digital image can be distinguished by their gray-level or colour values. This paper presents a new histogram based multi level threshold algorithm resulting in multilevel threshold values. This technique is based on individual value of histogram column. This new method consists of three steps. In the first stage, a hill-clustering technique is applied and peak locations of the histogram are

approximately determined. This technique is iterative and converging if the number of peaks found is less than or equal to the desirable maximum number of peaks. In the second stage, the histogram segments between the peaks are approximated by real rational function and the minimax criterion. The result of this method is the approximate valley points of the histogram. With this procedure, therefore, the histogram segments between the peaks get fitted. Finally, the multilevel threshold values of the histogram are defined as global minimum value of each rational function. To find these global optimal values, the one dimensional golden search algorithm is applied.

3.1.1. Peak Determination using Hill-Clustering Method

The hill-clustering method is used in this paper to find the peaks. A gray-level image contains objects and background. In an image, each object corresponds to a hill in the image histogram. The histogram of such an image is a nonnegative, real-valued function and contains peaks and valleys. Pixels that lie in the neighbourhood of peaks are classified as object pixels, whereas valley pixels are characterized as unclassified because they do not belong to a specific object.

Let R be the set of the positive integers representing the image gray levels, and $f(x, y)$ the image function giving the gray-level value of the pixel with the coordinates (x, y) . The histogram $H(k)$ of this image can be defined as:

$$H(k) = \sum_{\forall f(x,y)=k} f(x,y), \quad k \in R \quad (1)$$

The multilevel threshold selection can be considered as the problem of finding a set $T(k)$, $k = 1, 2, \dots, L$ of threshold values, in order that the original gray-level image would be transformed to a new one with only $L+1$ levels. More specifically, if $T(k)$, $k = 1, 2, \dots, k$, are the threshold values with T_1, T_2, \dots, T_L , then the output image can be defined as

$$F(x, y) = \begin{matrix} m_0, & \text{if } f(x, y) \leq T_1 \\ m_1, & \text{if } T_1 < f(x, y) \leq T_2 \\ \cdot & \\ \cdot & \\ \cdot & \\ m_L, & \text{if } f(x, y) \geq T_L \end{matrix} \quad (2)$$

where m_k represents the mean histogram values in the range (T_k, T_{k+1}) , with $T_0 = 0$ and $T_L = 255$.

In this multilevel threshold method the locations of the histogram peaks are determined using hill-clustering method, in which peaks can be approximately determined

by an iterative procedure. In each iteration the number of gray levels is reduced by half. This method consists of the following steps:

Step1. Give the value of N, where N is the maximum number of histogram peaks. The iterative clustering procedure converges when the total number of determined peaks is less than or equal to N. Also set ITR = 0

Step2. Set ITR = ITR+1 and the number of cells equal to $N_{C, ITR} = N_{cnt} / 2^{ITR-1}$, where N_{cnt} is the number of cells of the initial histogram. The frequency of each cell f_i is defined as,

$$g_{i, ITR} = \frac{1}{2}[g_{i, ITR-1} + g_{i-1, ITR}], i = 1, 2, \dots, N_{C, ITR}$$

Step3. Establish the arrow directions. If d_i is the arrow direction at cell i , then

$$d_i = \begin{cases} +1, & \text{if } (f_{i-1} > f_{i+1}) \cap (f_{i-1} \geq f_i) \neq 0 \\ -1, & \text{if } (f_{i+1} > f_{i-1}) \cap (f_{i+1} \geq f_i) \neq 0 \\ 0, & \text{otherwise} \end{cases}$$

In the case of tie ie., if $f_{i-1} = f_{i+1}$, set $d_i = d_{i-1}$

Step4. Identify the peaks:

- (i) if $(d_i = 0) \cap (d_{i-1} = -1) \cap (d_{i+1} = +1)$, then cell i is the peak of the hill; or
- (ii) If $(d_{i-1} = -1) \cap (d_{i+1} = +1)$, then a peak is also identified between cells i and $i+1$. Repeat step 4 to identify all peaks in the histogram

Step5. If the number of peaks identified in Step4 is less than or equal to the desired number of peaks, then go to Step6; otherwise go to Step2.

Step6. Approximate the locations of the histogram peaks and terminate the procedure. Specifically, if cell i is a peak then its gray level is identified as the location of the peak. The final number of peaks corresponds to the total number of hills and consequently to the total number of objects.

3.1.2. Multilevel Threshold Computation

The second stage of this method is the fitting of the histogram data between the peaks. Since N is the number of peaks, the histogram has N-1 valleys, which lie between peaks.

For the n_{th} valley let: K be the total number of gray levels included; $G(w_k)$, $k=1,2,\dots,K$, be the values of the histogram at the w_k level; W_k , $k=1,2,\dots,K$, be the gray level values, with $W_n \leq w_k \leq W_{n+1}$.

For each valley, fit the histogram points $(w_k, G(w_k))$, $k=1,2,\dots,K$ by a real rational function $R(w)$ of the general form

$$R(w) = \frac{A(w)}{B(w)} = \frac{\sum_{m=0}^N a_{mw}^m}{1 + \sum_{m=1}^M b_{mw}^m}, \quad (3)$$

where a_m and b_m are the unknown coefficients and, N and M are integers that define the degree of polynomials $A(w)$ and $B(w)$.

$R(w)$ is a real and continuous function. To find its minimum in the region $[W_n, W_{n+1}]$, the one dimensional golden search algorithm is applied. The inputs of the golden search algorithm are only the limits of the interval. In this case the limits are defined by the W_n and W_{n+1} , while the one-dimensional function for each region is the real rational function $R(w)$. The following procedure is used to ensure that the golden search algorithm always converges to the global minimum.

Step1. Find the minimum R_{min} of $R(w)$

Step2. Define the function $Y(w)$ according to the relation

$$Y(w) = \begin{cases} R(w) & \text{if } R(w) \leq R_{min} \\ R_{min} & \text{otherwise} \end{cases}$$

Step3. Find the minimum Y_{min} of $Y(w)$

Step4. If $Y_{min} = R_{min}$, go to Step5; otherwise put $R_{min} = Y_{min}$ and go to step2.

Step 5. The global minimum solution is equal to R_{min} . Terminate the procedure.

The result of the above minimization procedure is the minimum value of $R(w)$ and its position. This minimum is taken as a threshold value of the histogram.

The i_{th} threshold $T(i)$ is computed as

$$T(i) = P(i) + Min - 1,$$

where $P(i)$ is the i_{th} peak value and Min is the global minima [13,14,15].

4. Extraction And Localization Of Optic Disc

4.1 Preprocessing

4.1.1. Selection of Red Channel

The first stage in Pre-Processing steps is the colour space conversion. In this step the image is converted from an RGB image to a grayscale image. During this process, the RGB value of each pixel is replaced by the mean value of the green and blue values of the pixel [16].

4.1.2. Blood Vessel Removal

Blood vessel patches emanating from the optic nerve head covers large proportion of neuroretinal rim and their existence makes the analysis more difficult. The presence of blood vessels that run on the outline of the optic disc makes it difficult to extract OD accurately. Morphological closing method is used to remove the blood vessels of the retinal image. An 8 x 8 disc shaped structuring element is given the

formula of closing operation [17].

Closing:

$$I_s(R, B) = R \bullet B = E(D(R, -B), -B) \quad (4)$$

where R is the red channel of the input image and B is an 8x8 symmetrical disc structuring element, to remove the blood vessels[15]. I_s is the resultant vessel free, smoothed output image. Figure 2 shows the result of the preprocessing operation.

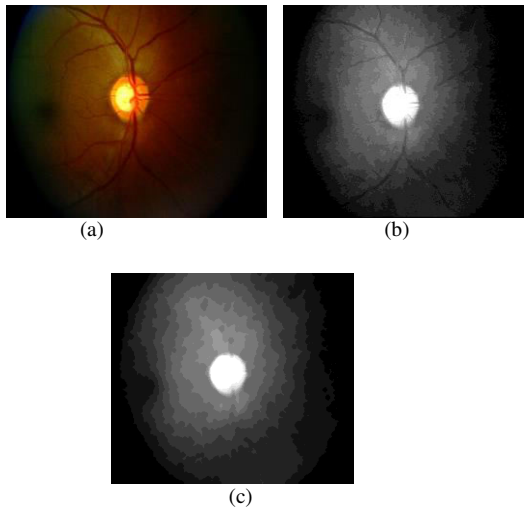


Figure2. (a) Input image (b) red channel of the input image (c) Vessel free image

4.1.3. Peak Determination and Histogram Fitting

In this paper 3 is the assigned value of the number of peaks. This algorithm generates a new number peaks for each image and the histogram is get fitted. In this test image for the given number of peaks 3. The peaks of the histogram are at: 8 32 80 96 184 240.

The following figure, Figure 3 shows the histogram fitting of peaks and thresholds.

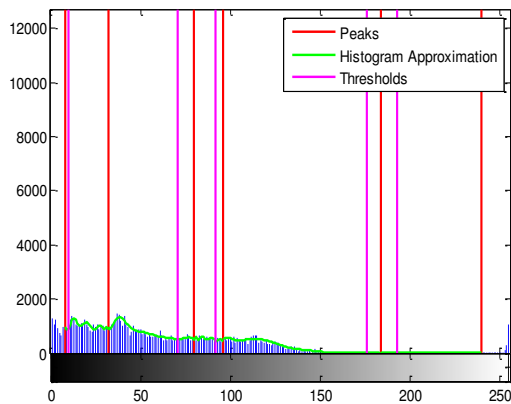


Figure 3 The histogram fitting of peaks and thresholds

4.1.4. Multilevel Thresholding

The multiple thresholds obtained are used for the thresholding operation of the vessel free image. In this test image he recommended number of thresholds is 5. The following figure, figure 4 depicts the image after multithresholding.

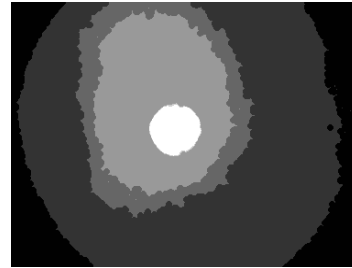


Figure4. Vessel free image after Multithresholding

4.1.5. Optic Disc Extraction

OD is the brightest feature in a normal fundus image and it has an elliptical shape. It appears bright orange-pink with a pale centre. Orange-pink appearance represents the healthy neuro-retinal tissue. From this segmented image the OD is extracted. Since the OD has the highest intensity, the image portion with highest threshold is used to extract OD. The highest threshold Tmax is computed using the following equation.

$$T_{max} = \text{Max}(T(i)), i=1, 2, \dots, k \quad (5)$$

where Tmax is the highest threshold, k is the total number of thresholds. In this test image highest threshold 240 is used for the extraction of OD. The erosion operation is applied to remove the unwanted objects from the extracted image. The extracted OD is given in figure 5.

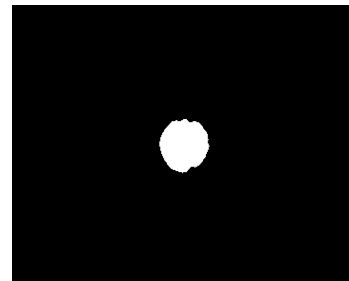


Figure 5 Extracted Optic Disc

4.1.6. Optic Disc Localization

Similarly, the centroid $[X1,Y1]$ of the extracted OD is computed as the average of the rows and columns of the extracted OD. The following equations are used to compute the X and Y coordinates of the centroid.

$$X1 = \frac{1}{M1} \sum_{i=1}^{M1} x_i \quad (6)$$

$$Y1 = \frac{1}{N1} \sum_{i=1}^{N1} y_i \quad (7)$$

where (x_i,y_i) is the coordinates, M1 is the number of rows and N1 is the number of columns of the boundary.

The obtained centroid is used to localize the OD of the input image. Figure 6 shows the OD localization of the test image.

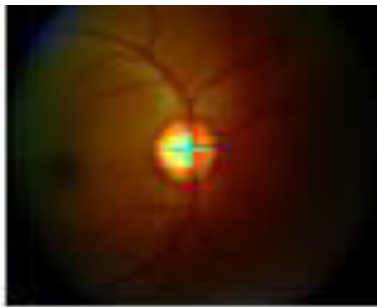


Figure6. Localization of Optic Disc on the Input Image

The centroid calculated by means of ground truth boundary of DRION database is used as the ground truth centroid for the images of DRION database. The centroid obtained from the ophthalmologist is used as the ground truth for the rest of the images.

The centroid of the ground truth boundary $[X,Y]$ is computed using the average of the rows and columns of the boundary. The following equations are used to compute the X and Y coordinates of the centroid.

$$X = \frac{1}{M} \sum_{i=1}^M x_i \quad (8)$$

$$Y = \frac{1}{N} \sum_{i=1}^N y_i \quad (9)$$

where (x_i,y_i) is the coordinates, M is the number of rows and N is the number of columns of the boundary.

Similarly, the centroid $[X1,Y1]$ of the extracted OD is computed as the average of the rows and columns of the extracted OD.

The following equations are used to compute the X and Y coordinates of the centroid.

$$X1 = \frac{1}{M1} \sum_{i=1}^{M1} x_i \quad (10)$$

$$Y1 = \frac{1}{N1} \sum_{i=1}^{N1} y_i \quad (11)$$

where (x_i,y_i) is the coordinates, M1 is the number of rows and N1 is the number of columns of the boundary.

The following figure 7 shows the centroid obtained using the ground truth boundary $[X ,Y] = (335.3123, 178.5210)$ and the centroid obtained using the extracted OD $[X1,Y1] = (335.5995, 178.5471)$ of a test image. From the result it is shown that both results are approximately same. Figure 7 shows the centroids obtained using the ground truth and the present method.

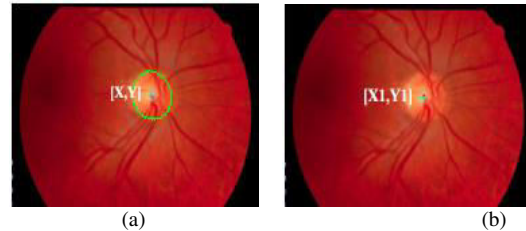


Figure 7(a) Centroid using the ground truth boundary (b) Centroid using the present method (Cross represents the OD center)

5. Results and Discussions

The new method was tested on the publically available databases DRION, DIARETDB0 and DIARETDB1 and images obtained from an ophthalmologist. The success rate is as follows. Among the 110 images from DRION 105 images, among the 130 images from DIARETDB0 126 images, among the 86 images from DIARETDB1 84 images and among 75 images from the ophthalmologist 75 images were success fully extracted and localized OD.

5.1. Retinal Image Databases

5.1.1 The DIARETDB0 and DIARETDB1 Databases

The DIARETDB0 and DIARETDB1 Database images were captured using an FOV of 50° and the size of each image is 1500 x 1152 x 3. Out of the 130 images of the DIARETDB0 database, 20 have normal architecture and 110 have various types of pathology. Out of the 89 images of the DIARETDB1 database, 5 have normal architecture and 84 have various types of pathology.

5.1.2. DRION database

It has 110 retinal images with each image having the resolution of 600 x 400 pixels and the optic disc annotated by two experts with 36 landmarks. The mean age of the patients was 53.0 years (standard Deviation 13.05), with 46.2% male and 53.8% female and all of them were Caucasian ethnicity 23.1% patients had chronic simple glaucoma and 76.9% eye hypertension. The images were acquired with a colour analogical fundus camera, approximately centered on the ONH and they were stored in slide format. In order to have the images in digital format, they were digitized using a HP-PhotoSmart-S20 high-resolution scanner, RGB format, resolution 600x400 and 8 bits/pixel. Independent contours from 2 medical

experts were collected by using a software tool provided for image annotation. In each image, each expert traced the contour by selecting the most significant papillary contour points and the annotation tool connected automatically adjacent points by a curve. The expert traced the contour of this dataset is used as the ground truth to facilitate the performance analysis using the comparison of the center of this contour with the center of the extracted OD.

5.1.3 Images from the ophthalmologist

The fundus images used in this experiment were taken from Giridhar Eye Institute, Kochi, Kerala. The size of the image is 576 x 768 x 3. All the images were obtained using Carlzeiss fundus camera. Out of 75 images, 5 are normal and 70 are glaucomatous.

5.2. Implementation

The present method was tested using 404 images obtained from the above mentioned databases and ophthalmologist. The method was evaluated by applying it to fundus images having different types of histograms. Figure 8 shows the results of histogram based multilevel thresholding of real images of varying OD size and shape. 5 Sample images from DIARETDB0, DIARETDB1, DRION-DB and Ophthalmologist and the centroid of the images are given in the following figure 8(a) and 8(b).

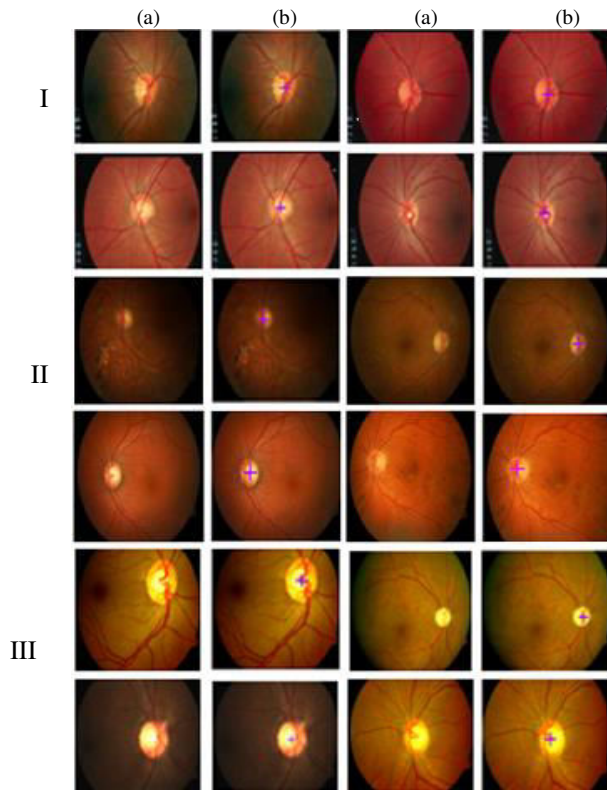


Figure 8 (a) Input Image (b) OD Localisation
 I – DRION, II - DIARETDB0 & DIARETDB1,
 III – Images from the ophthalmologist

5.3. Performance Evaluation

The performance evaluation is done using the following parameters.

5.3.1 Success rate

The decision for successful localization or failed localization is based on human eye observation. Table 2 shows the success rate of OD extraction using 404 images.

Table1. Success Rate Table

Database	Total Number of Images	Successful Localisation	Success Rate	Computation Time
Diaretdb0	130	126	96.92	3.18083
Diaretdb1	89	84	94.38	3.15385
Drion	110	105	95.45	3.28119
Ophthalmologist	75	75	100.00	3.41804
Total	404	390	96.69 (Average)	3.25848 (Average)

5.3.2 Accuracy

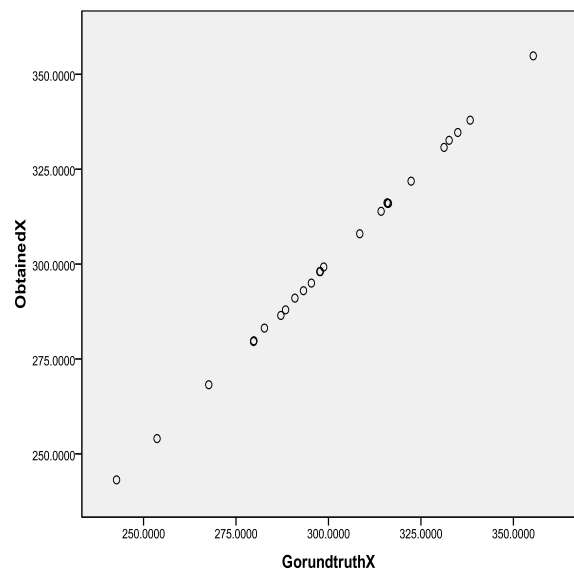
In order to evaluate the accuracy of the new algorithm, the comparison between the ground truth centroid and the obtained centroid is used. The centroid using the ground truth boundary obtained by an expert ophthalmologist from the DRION database is used as the ground truth centroid. For the other images the centroid obtained from an ophthalmologist is used for evaluation. The accuracy of the new technique is evaluated using the comparison of the centroid of the obtained OD with that of the centroid obtained using the ground truth boundary from the ophthalmologist. The centroid of 25 test images from DRION database and the corresponding obtained centroid are given in Table 1. From the table it is obvious that the mean difference of x- coordinate is only 0.3454 and the mean difference of y- coordinate is only 0.4405.

Table 2 Ground Truth and Obtained Centroid Comparison

<i>Image Name</i>	<i>Ground Truth X (1)</i>	<i>Obtained X1 (2)</i>	<i>Difference (X-X1) (1)-(2)</i>	<i>Ground Truth Y (3)</i>	<i>Obtained Y1 (4)</i>	<i>Difference (Y-Y1) (3)-(4)</i>
Im1	293.2462	292.9850	0.2612	219.5780	219.1659	0.4121
Im2	279.7386	279.5892	0.1494	228.9630	228.7508	0.2122
Im3	355.3641	354.8462	0.5179	206.7352	206.3748	0.3604
Im4	334.9644	334.6623	0.3021	213.3865	212.8562	0.5303
Im5	322.3469	321.8316	0.5153	242.1611	241.7773	0.3838
Im6	308.4632	307.9865	0.4767	217.9691	217.9805	0.0114
Im7	279.8240	279.7979	0.0261	215.9897	215.6577	0.3320
Im8	316.2130	316.0029	0.2101	223.8279	224.0279	0.2000
Im9	315.8531	316.1319	0.2788	205.7907	206.3391	0.5484
Im10	288.4020	287.9386	0.4634	176.6244	177.2155	0.5911
Im11	314.2352	313.8941	0.3411	212.3454	211.3843	0.9611
Im12	297.6687	298.0131	0.3444	214.3045	215.0327	0.7282
Im1 3	282.6848	283.1265	0.4417	238.8594	239.3447	0.4853
Im14	295.3830	294.9862	0.3968	191.6893	191.2451	0.4442
Im1 5	331.2497	330.7309	0.5188	197.5462	198.0346	0.4884
Im16	290.9223	291.0261	0.1038	191.0208	190.9564	0.0644
Im17	287.1293	286.4673	0.6620	200.1131	199.8435	0.2696
Im18	338.3123	337.8995	0.4128	179.5210	178.5471	0.7739
Im18	242.7048	243.1564	0.4516	205.1935	204.5118	0.6817
Im20	253.6553	254.0287	0.3734	208.0220	207.4397	0.5823
Im21	316.0102	315.9878	0.0224	217.8105	217.9705	0.1600
Im22	267.6372	268.2132	0.5760	221.0484	220.6725	0.3759
Im23	298.7078	299.2311	0.5233	217.8592	218.5172	0.6580
Im24	332.6179	332.5943	0.0236	203.7719	203.6952	0.0767
Im25	297.7823	298.0254	0.2431	219.4834	218.8032	0.6802
Mean Difference of X			0.3454	Mean Difference of Y		0.4405

5.3.3. Scatter plot Analysis

The statistical analysis is done using the scatter plot diagram. The ground truth x- coordinate(X) and the obtained x-coordinate(X1) and, the ground truth y- coordinate(Y) and obtained y-coordinate (Y1) of the centroids are plotted using the scatter plot diagram. From the scatter plot it is clear that there exists a highly positive linear relationship between both centroids. Figure 9(a) and Figure 9(b) depict the comparison between the x- coordinates and the y- coordinates of the ground truth and the obtained centroids.



(a)

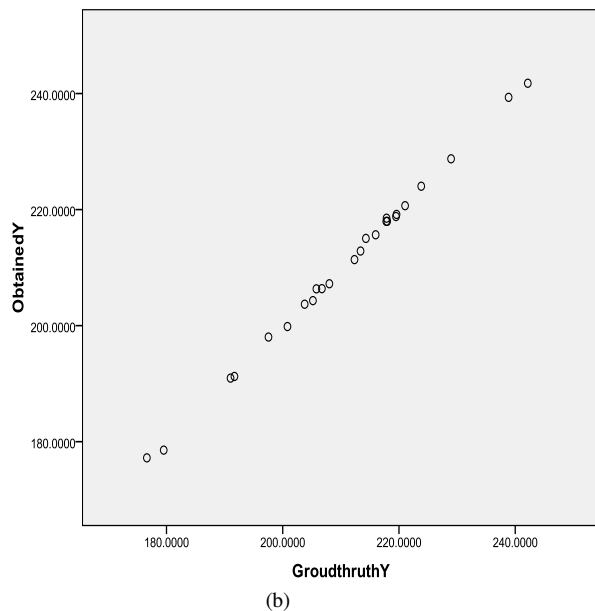


Figure 9. Scatter plot diagram shows the comparison of (a) ground truth $X(X1)$ and obtained $X(X2)$ (b) ground truth $Y(Y1)$ and obtained $Y(Y2)$

6. Conclusion

Automated extraction of optic disk parameters can be a valuable diagnostic-assisting resource for screening retinal images. This paper provides an efficient algorithm for the optic disc extraction and localization. Histogram based multilevel threshold algorithm is used here for the automatic extraction of OD. The centroid of the obtained OD is used to check the success or failure of the automatic extraction. The experimental results show that 96.69% disk localization can be done successfully by the present method out of the 404 testing images. The scatter plot diagram shows highly positive correlation between the ground truth OD center and obtained OD center. The failure occurs in certain high contrast images. Further study using advanced segmentation technique is needed to overcome this limitation. However, this automatic extraction method would help ophthalmologists to do retinal screening easily and quickly.

References

- [1] J. Hayashi, T. Kunieda, J. Cole, et al., "A Development of Computer-aided Diagnosis System Using Fundus Images", in H. Thwaites and L. Addison (ed), Proc. 7th VSMM, Los Alamitos, (1999), pp.429-438
- [2] Hoover, A., Goldbaum, M., "Locating the optic nerve in a retinal image using the fuzzy convergence of bloodvessels", IEEE Transactionson MedicalImaging, Vol.22, Issue:8 Aug. 2003, pp.951 - 958 .
- [3] H. Li and O. Chutatape, "A model-based approach for automated feature extraction in fundus images," IEEE Trans. Biomedical Engineering, Vol. 51(2), 2004, pp. 246–254.
- [4] J. Lowell, A. Hunter, D. Steel, A. Basu, R. Ryder, E. Fletcher, and L. Kennedy, "Optic nerve head segmentation," IEEE Trans. Medical Imaging, Vol. 23(2), 2004pp. 256–264.
- [5] Chrastek R., Wolf M., Donath K., Niemann H., Paulus D., Hothorn T., Lausen B., Lammer R., Mardin C.Y., Michelson G. "Automated Segmentation of the Optic Nerve Head for Diagnosis of Glaucoma", Medical Image Analysis, Vol.9, 2005, pp. 297-314.
- [6] Seng Soon Lee, Mandava Rajeswari, Dhanesh Ramachandram , "Preliminary and multi features localization of optic disc in color fundus images", National Computer Science Postgraduate Colloquium, (NaCSPC '05), 2005.
- [7] Yandong Tang et al, " Automatic segmentation of the papilla in a fundus image based on the CV model and a shape restraint", Proceedings of the 18th International Conference on pattern Recognition,2006.
- [8] Virance Thongnuch and Bunyyarit Uyyanonvara, "Automatic optic disc detection from low contrast retinal images of ROP infant using GVF snake", Suranaree Journal of Science Technology, Vol. 14, No.3, 2007,pp. 223-234.
- [9] J. Xu, O. Chutatape, E. Sung, C. Zheng, and P. Chew, "Optic disk feature extraction via modified deformable model technique for glaucoma analysis," Pattern Recognition, Vol. 40(7),2007 pp. 2063–2076.
- [10] D. Wong, J. Liu, J. Lim, X. Jia, F. Yin, H. Li, and T.Wong, "Level-set based automatic cup-to-disc ratio determination using retinal fundus images in argali", Proc. EMBC, 2008, pp. 2266–2269.
- [11] Jun Cheng ,Jiang Liu ,Wong, D.W.K. , Fengshou Yin , " Automatic optic disc segmentation with peripapillary atrophy elimination", Proc. EMBC, Annual Conference, IEEE, Aug. 30 - Sept. 3 2011, pp. 6224 – 6227.
- [12] Handayani Tjandrasa, Ari Wijayanti, Nanik Suciati , "Optic Nerve Head Segmentation Using Hough Transform and Active Contours", TELKOMNIKA, Vol.10, No.3, July 2012, pp. 531~536.
- [13] Dimo Dimov, and Lasko Laskov, "Cyclic Histogram Thresholding and Multithresholding", International Conference on Computer Systems and Technologies - CompSysTech'09,2009, Proc. Pp. II.5-1 - II.5-8
- [14] N. Papamarkose, B.Gatos, "A new approach for

multilevel threshold selection”, Graphical Models and Image Processing, Vol. 56, No.5, September,1994, pp.357-370.

- [15] Zhengjian DING., Juanjuan JIA, Dai LI, “Fast Clustering Segmentation Method Combining Hill-climbing for Color Image”, Journal of Information & Computational Science 8: 14, 2011,pp.2949–2957.
- [16] Rafael C Gonzalez, Richard E Woods, Steven L Eddins, Digital Image Processing, Prentice Hall Publications, 2009.
- [17] Rafael C Gonzalez, Richard E Woods, Steven L Eddins., Digital Image Processing Using Matlab, Prentice Hall Publications, 2009.

Thresiamma Devasia was graduated with bachelor of Mathematics (BSc.Maths) from Mahatma University, Kerala, India in 1991, and finished her master of computer applications (MCA) and M.Phil Computer Science from Alagappa University Tamilnadu, India in 1995 and 2010, respectively. Currently, she is the Head of the Department and Associate professor, Department of Computer Science, Assumption College Changanacherry, Kerala, India and working toward her Ph.D. at Cochin University of Science And Technology on glaucoma detection using image processing. She completed UGC sponsored minor research project based on image processing. She was a member of IEEE. Her interest areas include image processing and medical imaging.

Dr. K.Poulose Jacob, Professor of Computer Science at Cochin University of Science and Technology since 1994, is currently Pro Vice Chancellor of Cochin University of Science & Technology. He has presented research papers in several International Conferences in Europe, USA, UK, Australia and other countries. He has served as a Member of the Standing Committee of the UGC on Computer Education & Development. He is the Zonal Coordinator of the DOEACC Society under the Ministry of Information Technology, Government of India. He serves as a member of the AICTE expert panel for accreditation and approval. He has been a member of several academic bodies of different Universities and Institutes. He is on the editorial board of two international journals in Computer Science. Dr. K.Poulose Jacob is a Professional member of the ACM (Association for Computing Machinery) and a Life Member of the Computer Society of India.

Dr.Tessamma Thomas received her M.Tech. and Ph.D from Cochin University of Science and Technology, Cochin-22, India. At present she is working as Professor in the Department of Electronics, Cochin University of Science and Technology. She has to her credit more than 100 research papers, in various research fields, published in International and National journals and conferences. Her areas of interest include digital signal / image processing, bio medical image processing, super resolution, content based image retrieval, genomic signal processing, etc.